Centrum Wiskunde & Informatica

Imaging the Acoustic and Optical Properties of the Breast with USCT and PAT

Felix Lucka

SIAM Imaging Science
8th July 2020

Quantitative Photoacoustic Breast Imaging

- hybrid imaging: "light in, sound out"
- non-ionizing, near-infrared radiation
- quantitative images of optical properties
- novel diagnostic information

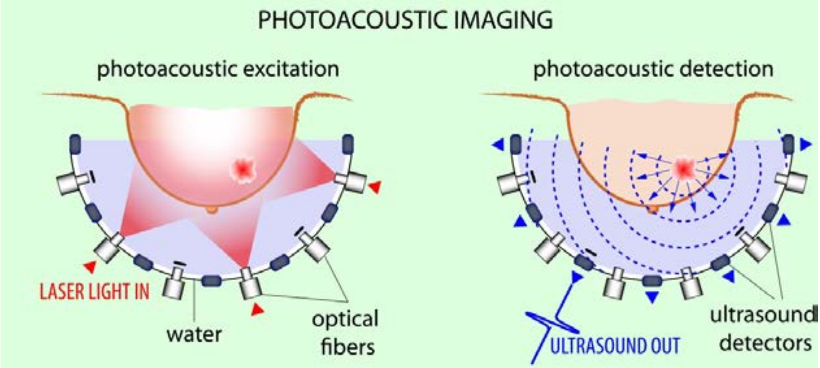

Photoacoustic Imaging: Spectral Properties

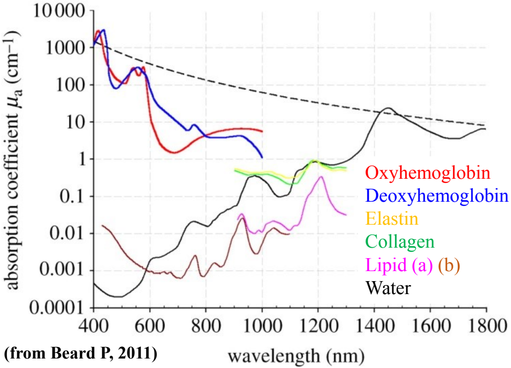

- different wavelengths allow quantitative spectroscopic examinations.
- gap between oxygenated and deoxygenated blood.

Quantitative Ultrasonic Breast Imaging

- "sound in, sound out"
- different from conventional US but as safe
- quantitative images of acoustic properties
- novel diagnostic information

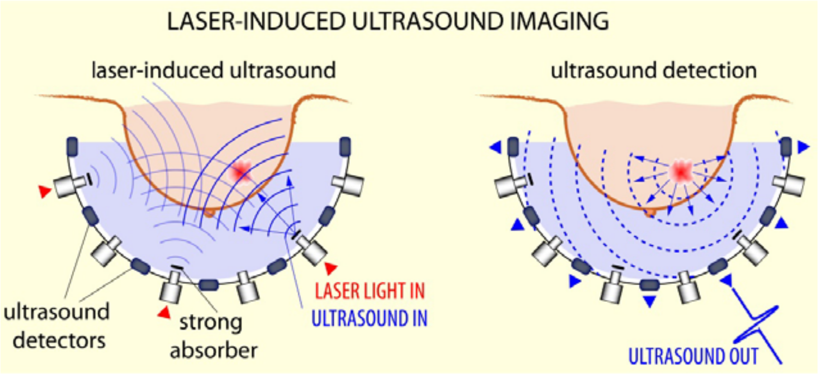

H2020 Project: Novel PAT+USCT Mammography Scanner

Novel diagnostic information from optical and acoustic properties

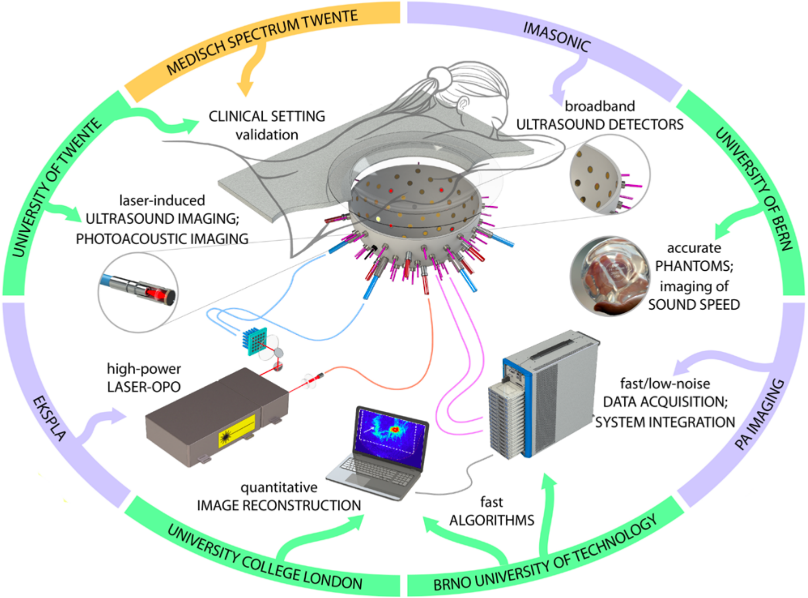

Our Contributions

- simulation studies for
  - ultrasonic transducer specification
  - light excitation design
  - sensing pattern design
  - measurement protocol design
- reconstruction algorithm design:
  - accuracy vs. computational time/resources/complexity
  - scanner modelling
  - assist high performance computing implementation
- assist phantom design
- assist calibration measurement design
- process data, refine measurement procedures

Mathematical Modelling (simplified)

Quantitative Photoacoustic Tomography (QPAT)

radiative transfer equation (RTE) + acoustic wave equation

$$(v \cdot \nabla + \mu_a(x) + \mu_s(x))\,\phi(x,v) = q(x,v) + \mu_s(x)\int \Theta(v,v')\phi(x,v')dv',$$

$$p^{PA}(x,t=0) = p_0 := \Gamma(x)\mu_a(x)\int \phi(x,v)dv, \qquad \partial_t p^{PA}(x,t=0) = 0$$

$$(c(x)^{-2}\partial_t^2 - \Delta)p^{PA}(x,t) = 0, \qquad f^{PA} = Mp^{PA}$$

Ultrasound Computed Tomography (USCT)

$$(c(x)^{-2}\partial_t^2 - \Delta)p_i^{US}(x,t) = s_i(x,t), \qquad f_i^{US} = M_i p_i^{US} \qquad i = 1,\dots,n_{src}$$

Step-by-step inversion

1. $f^{US} \to c$: acoustic parameter identification from boundary data.
2. $f^{PA} \to p_0$: acoustic initial value problem with boundary data.
3. $p_0 \to \mu_a$: optical parameter identification from internal data.

USCT Reconstruction Approaches

$$({\color{teal}c(x)}^{-2}\partial_t^2 - \Delta)p_i^{US}(x,t) = s_i(x,t), \qquad f_i^{US} = M_i p_i^{US} \qquad i = 1,\ldots,n_{src}$$

Travel time tomography: geometrical optics approximation.

- ✓ robust & computationally efficient
- ! valid for high frequencies (attenuation!), low res, lots of data

Reverse time migration: forward wavefield correlated in time with backward wavefield (adjoint wave equation) via imaging condition

- ✓ 2 wave simulations, better quality
- ! approximation, needs initial guess, quantitative errors

Full waveform inversion (FWI): fit full model to all data.

- ✓ high res from little data, transducer modelling, constraints
- ! many wave simulations, complex numerical optimization
- low TRL but already used in 2D systems

Time Domain Full Waveform Inversion

$$F(c)p_i := (c^{-2}\partial_t^2 - \Delta)p_i = s_i, \qquad f_i = M_i\, p_i, \quad i = 1, \ldots, n_{src}$$

$$\min_{c \in \mathcal{C}} \sum_i^{n_{src}} \mathcal{D}\left(f_i(c), f_i^\delta\right) \quad s.t. \quad f_i(c) = M_i F^{-1}(c) s_i$$

gradient for **first-order optimization** via **adjoint state method**:

$$\nabla_c \mathcal{D}\left(f(c), f^\delta\right) = 2 \int_0^T \frac{1}{c(x)^3} \left(\frac{\partial^2 p(x,t)}{\partial t^2}\right) q^*(x,t) \quad ,$$

where $(c^{-2}\partial_t^2 - \Delta)q^* = s^*$, $s^*(x,t)$ is time-reversed data discrepancy

$\rightarrow$ **two wave simulations for one gradient**

Starting point in 2D:

Pérez-Liva, Herraiz, Udías, Miller, Cox, Treeby 2017. Time domain reconstruction of sound speed and attenuation in ultrasound computed tomography using full wave inversion, *JASA*.

3D Time Domain FWI for Breast USCT

$$\min_{c \in \mathcal{C}} \sum_{i}^{n_{src}} \mathcal{D}\left(M_i F^{-1}(c) s_i, f_i^{\delta}\right)$$

$$\nabla_c \mathcal{D}\left(f(c), f^{\delta}\right) = 2 \int_0^T \frac{1}{c(x)^3} \left(\frac{\partial^2 p(x,t)}{\partial t^2}\right) q^*(x,t)$$

Challenges and solutions for 3D:

- **!** 2 x n_{src} wave simulations per gradient
- **!** computationally & stochastically efficient gradient estimator
- **!** memory requirements of gradient computation
- **!** slow convergence and local minima
- **!** computational resources

3D Time Domain FWI for Breast USCT

$$\min_{c \in \mathcal{C}} \sum_{i}^{n_{src}} \mathcal{D}\left(M_i F^{-1}(c) s_i, f_i^\delta\right)$$

$$\nabla_c \mathcal{D}\left(f(c), f^\delta\right) = 2 \int_0^T \frac{1}{c(x)^3} \left(\frac{\partial^2 p(x,t)}{\partial t^2}\right) q^*(x,t)$$

Challenges and solutions for 3D:

! 2 x n_{src} wave simulations per gradient
$\longrightarrow$ **stochastic quasi-newton optimization (SL-BFGS)**

! computationally & stochastically efficient gradient estimator

! memory requirements of gradient computation

! slow convergence and local minima

! computational resources

3D Time Domain FWI for Breast USCT

$$\min_{c \in \mathcal{C}} \sum_{i}^{n_{src}} \mathcal{D}\left(M_i F^{-1}(c) s_i, f_i^\delta\right)$$

$$\nabla_c \mathcal{D}\left(f(c), f^\delta\right) = 2 \int_0^T \frac{1}{c(x)^3} \left(\frac{\partial^2 p(x,t)}{\partial t^2}\right) q^*(x,t)$$

Challenges and solutions for 3D:

! 2 x n_{src} wave simulations per gradient

$\longrightarrow$ **stochastic quasi-newton optimization (SL-BFGS)**

! computationally & stochastically efficient gradient estimator

$\longrightarrow$ **source encoding for time-invariant systems**

! memory requirements of gradient computation

! slow convergence and local minima

! computational resources

3D Time Domain FWI for Breast USCT

$$\min_{c \in \mathcal{C}} \sum_{i}^{n_{src}} \mathcal{D}\left(M_i F^{-1}(c) s_i, f_i^\delta\right)$$

$$\nabla_c \mathcal{D}\left(f(c), f^\delta\right) = 2 \int_0^T \frac{1}{c(x)^3} \left(\frac{\partial^2 p(x,t)}{\partial t^2}\right) q^*(x,t)$$

Challenges and solutions for 3D:

- ! 2 x n_{src} wave simulations per gradient
  $\longrightarrow$ **stochastic quasi-newton optimization (SL-BFGS)**
- ! computationally & stochastically efficient gradient estimator
  $\longrightarrow$ **source encoding for time-invariant systems**
- ! memory requirements of gradient computation
  $\longrightarrow$ **time-reversal based gradient computation**
- ! slow convergence and local minima

- ! computational resources

3D Time Domain FWI for Breast USCT

$$\min_{c \in \mathcal{C}} \sum_{i}^{n_{src}} \mathcal{D}\left(M_i F^{-1}(c) s_i, f_i^\delta\right)$$

$$\nabla_c \mathcal{D}\left(f(c), f^\delta\right) = 2 \int_0^T \frac{1}{c(x)^3} \left(\frac{\partial^2 p(x,t)}{\partial t^2}\right) q^*(x,t)$$

Challenges and solutions for 3D:

- **!** 2 x n_{src} wave simulations per gradient
  $\longrightarrow$ **stochastic quasi-newton optimization (SL-BFGS)**
- **!** computationally & stochastically efficient gradient estimator
  $\longrightarrow$ **source encoding for time-invariant systems**
- **!** memory requirements of gradient computation
  $\longrightarrow$ **time-reversal based gradient computation**
- **!** slow convergence and local minima
  $\longrightarrow$ **coarse-to-fine multigrid schemes**
- **!** computational resources

3D Time Domain FWI for Breast USCT

$$\min_{c \in \mathcal{C}} \sum_{i}^{n_{src}} \mathcal{D}\left(M_i F^{-1}(c) s_i, f_i^\delta\right)$$

$$\nabla_c \mathcal{D}\left(f(c), f^\delta\right) = 2 \int_0^T \frac{1}{c(x)^3} \left(\frac{\partial^2 p(x,t)}{\partial t^2}\right) q^*(x,t)$$

Challenges and solutions for 3D:

- ! 2 x n_{src} wave simulations per gradient
  $\longrightarrow$ **stochastic quasi-newton optimization (SL-BFGS)**
- ! computationally & stochastically efficient gradient estimator
  $\longrightarrow$ **source encoding for time-invariant systems**
- ! memory requirements of gradient computation
  $\longrightarrow$ **time-reversal based gradient computation**
- ! slow convergence and local minima
  $\longrightarrow$ **coarse-to-fine multigrid schemes**
- ! computational resources
  $\longrightarrow$ **runs on single GPU, can utilize multiple GPUs**

3D FWI: Setup

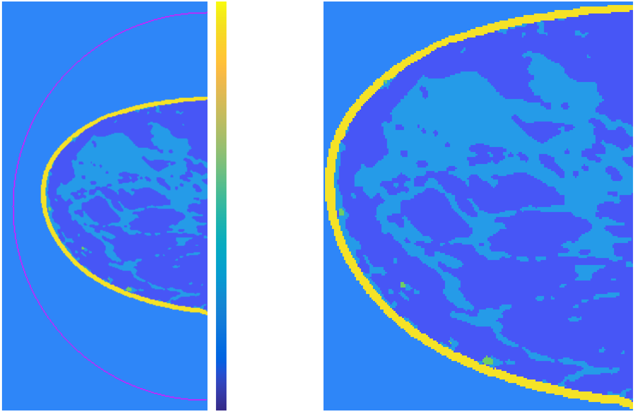

- color range 1435-1665 m/s
- 3D breast phantom at 0.5mm resolution, 1024 sources and receivers
- $442 \times 442 \times 222$ voxel, 3912 time steps

Yang Lou et al. Generation of anatomically realistic numerical phantoms for photoacoustic and ultrasonic breast imaging, *JBO, 2017.*

3D FWI: Initialization

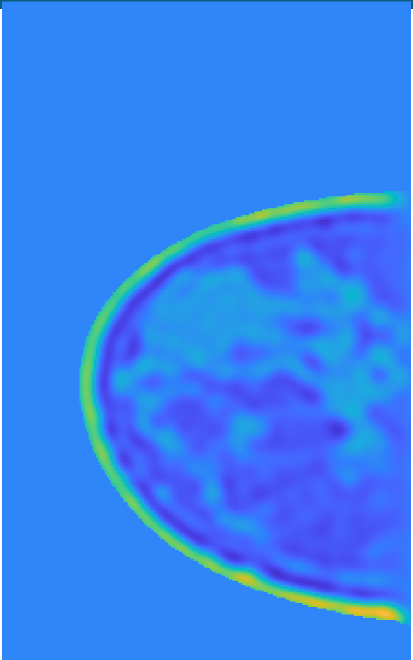

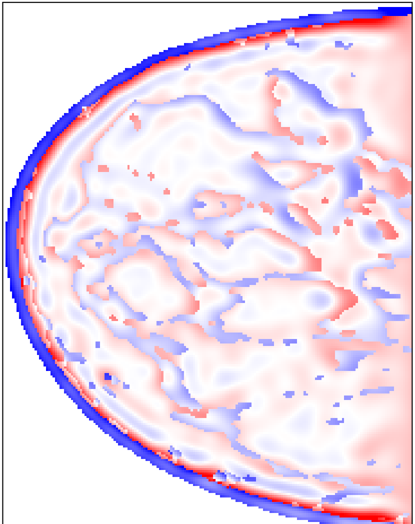

3D FWI: 32 Gradient Evaluations (16h, single GPU)

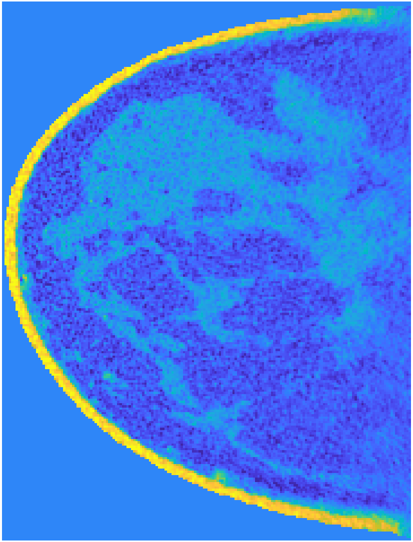

sound speed
(color range 1435 to 1665 m/s)

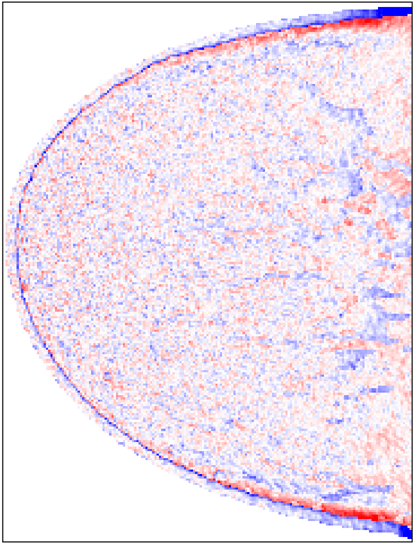

error
(color range -100 to +100 m/s)

3D FWI: 64 Gradient Evaluations (32h, single GPU)

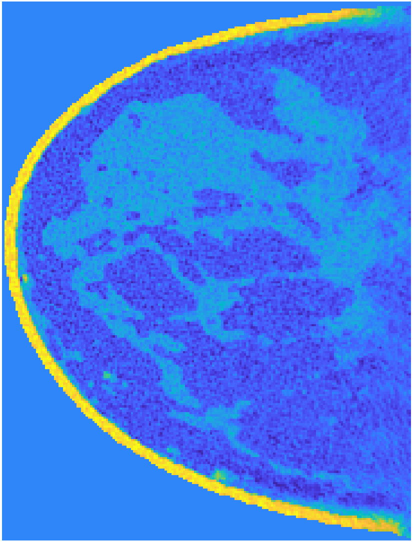

sound speed
(color range 1435 to 1665 m/s)

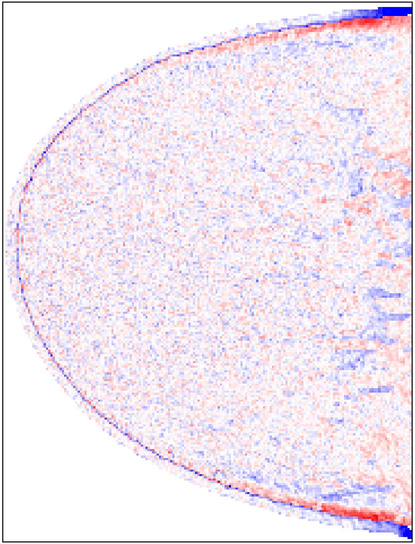

error
(color range -100 to +100 m/s)

3D FWI: 128 Gradient Evaluations (64h, single GPU)

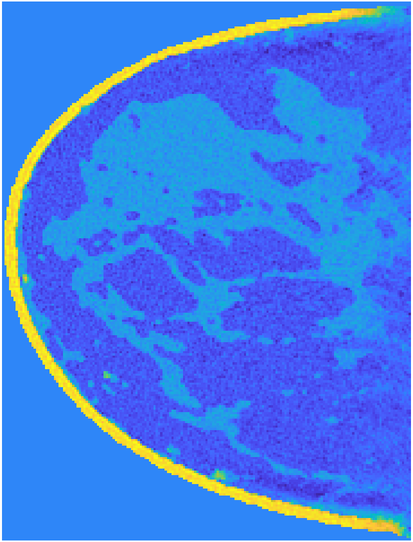

sound speed
(color range 1435 to 1665 m/s)

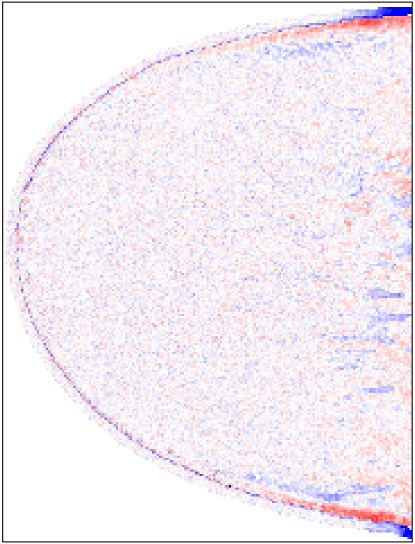

error
(color range -100 to +100 m/s)

3D FWI: Depth vs Error Distribution

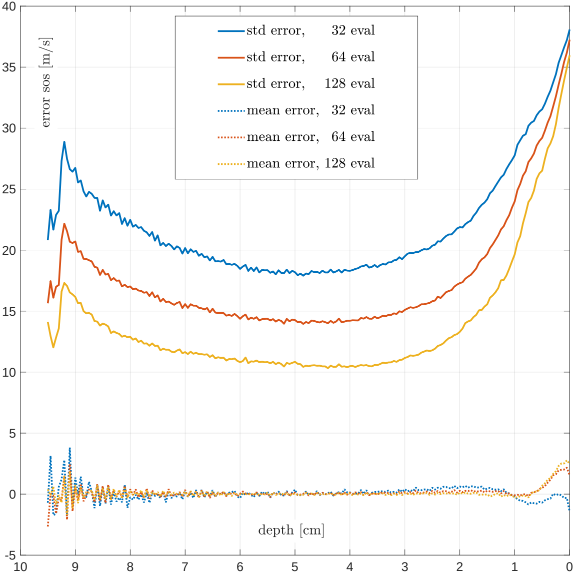

3D FWI in 24h on desktop with single GPU

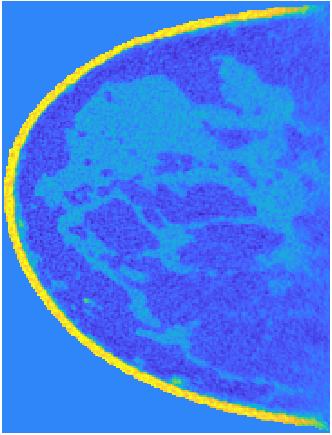

color range 1435 to 1665 m/s

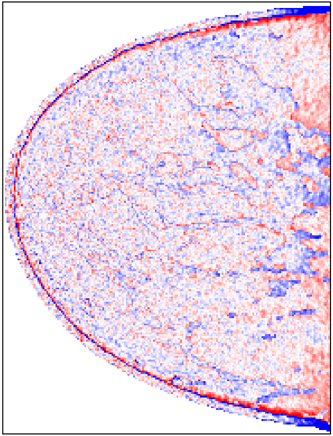

color range -50 to +50 m/s

- multi-grid with 3 level, coarsening factor 2
- SL-BFGS, slowness transform, prog. iter averaging
- time-reversal based source encoding gradient estimator

3D FWI in 24h on cluster with 4 GPU

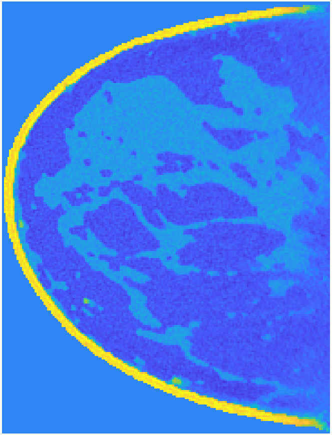

color range 1435 to 1665 m/s

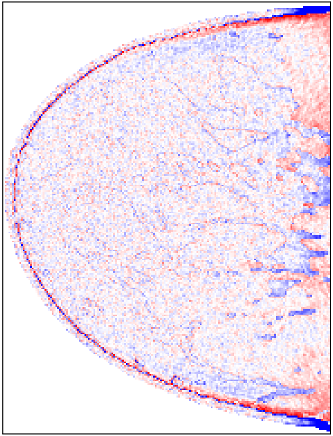

color range -50 to +50 m/s

- multi-grid with 3 level, coarsening factor 2
- SL-BFGS, slowness transform, prog. iter averaging
- time-reversal based source encoding gradient estimator

3D FWI in 24h on cluster with 16 GPU

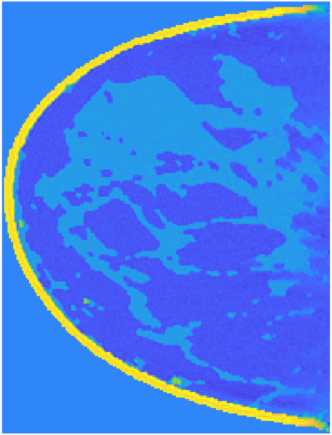

color range 1435 to 1665 m/s

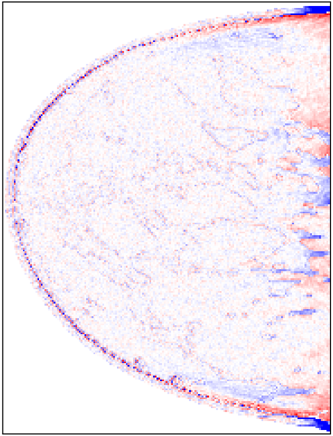

color range -50 to +50 m/s

- multi-grid with 3 level, coarsening factor 2
- SL-BFGS, slowness transform, prog. iter averaging
- time-reversal based source encoding gradient estimator

Reconstruction of Initial Photoacoustic Pressure

$$(c(x)^{-2}\partial_t^2 - \Delta)p^{PA}(x,t) = 0, \quad p^{PA}(x, t=0) = p_0, \quad f^{PA} = Mp^{PA}$$

$$f^{PA} = MAp_0$$

$$\hat{p}_0 = \operatorname*{argmin}_{p_0 \in \mathcal{C}} \left\| MAp_0 - f^{PA} \right\|_2^2 + \mathcal{R}(p_0)$$

- ✓ linear inverse problem
- ✓ variational approach
- ✓ first order optimization with early stopping
- **!** model acoustic properties
- **!** acquisition model discrepancies: laser excitation, rotation
- **!** model /calibrate piezoelectric sensor properties: impulse response, angular sensitivity, ...

Arridge, Betcke, Cox, L, Treeby, 2016. On the Adjoint Operator in Photoacoustic Tomography, *Inverse Problems 32(11).*

Optical & Spectral Inversion: Overview

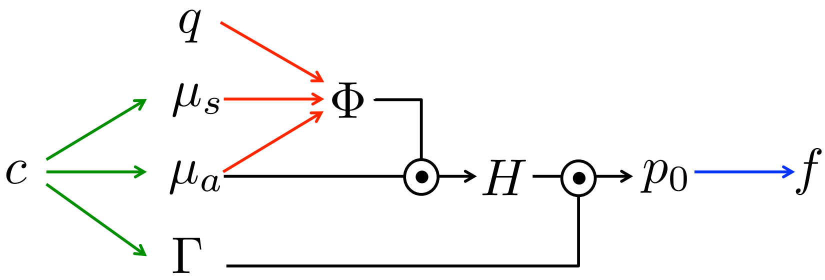

- mapping from c to (μ_a, μ_s, Γ): spectra?
- q: light source properties?
- mapping from (μ_a, μ_s, q) to Φ: non-linear.

The RTE and Toast++

Radiative transfer equation

$$(v \cdot \nabla + \mu_a(x) + \mu_s(x))\,\phi(x,v) = q(x,v) + \mu_s(x)\int \Theta(v,v')\phi(x,v')dv'$$

$$\Phi(x) = \int \phi(x,v)dv, \qquad\qquad \textbf{!}\ (x,v) \in \mathbb{R}^5 \rightsquigarrow \text{direct FEM infeasible.}$$

Diffusion approximation

$$(\mu_a(x) - \nabla \cdot \kappa(x)\nabla)\,\Phi(x) = \int q(x,v)dv, \quad \kappa = \frac{1}{\nu(\mu_a + \mu_s(1-g))}$$

source modelling? diffusivity matching?

Toast++

Schweiger, Arridge, 2014. The Toast++ software suite for forward and inverse modeling in optical tomography, *Journal of Biomedical Optics.*

Model Based Inversion

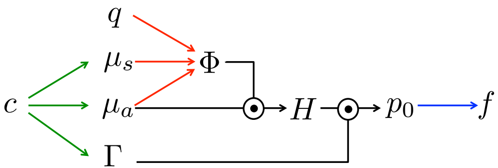

$$\hat{c} = \underset{c \in \mathcal{C}}{\operatorname{argmin}} \sum_{\lambda=1}^{N_\lambda} \int_{ROI} \left(p_{0,\lambda}^{recon} - p_{0,\lambda}(c)\right)^2 dx$$

- solve via iterative first order method (L-BFGS)
- derivatives of $\Phi(\mu_a, \mu_s)$ via adjoint method: two solves of light model per iteration (per wavelength).
- grid/mesh interpolation

Malone, Powell, Cox, Arridge, 2015. Reconstruction-classification method for quantitative photoacoustic tomography, *JBO.*

We Have Done This Before?

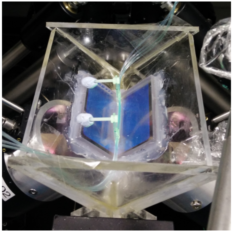

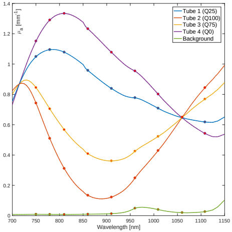

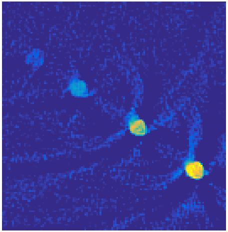

- well-controlled laboratory experiment
- full characterization of optical, acoustic and thermoelastic properties of phantom (sO_2 analogue)
- examined sensitivities, computational aspects, etc.
- promising results but a lot to improve

Fonseca, Malone, L, Ellwood, An, Arridge, Beard, Cox, 2017.
Three-dimensional photoacoustic imaging and inversion for accurate quantification of chromophore distributions, *Proc. SPIE 2017.*

Optical Parameters of Biological Tissues

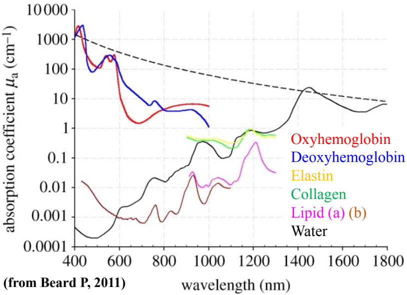

(from Beard P, 2011)

- based on different studies with different techniques
- mix of model assumptions and measurements
- often aimed at providing "somewhat" realistic values for simulations, not precise values for inversion
- the more you read about it, the less confident you get

Jacques, 2013. Optical properties of biological tissues: A review, *Phys. Med. Biol.*

Summary

Mammography scanner:

- novel diagnostic information from optical and acoustic properties
- high res, quantitative, deep into the breast
- 5 years of design, specification, component improvement
- things are coming together, stress levels are rising...

3D USCT:

- proof-of-concept studies of TD-FWI for high res 3D USCT in < 24h
- stochastic L-BFGS with source encoding
- time reversal based gradient computation
- multi-grid initialization

3D QPAT:

- we'll see how far we get :)

L, Pérez-Liva, Treeby, Cox, 2020. Time-Domain Full Waveform Inversion for High Resolution 3D Ultrasound Computed Tomography of the Breast, *in preparation.*

Fonseca, Malone, L, Ellwood, An, Arridge, Beard, Cox, 2017. Three-dimensional photoacoustic imaging and inversion for accurate quantification of chromophore distributions, *Proc. SPIE 2017.*

PHOTONICS PUBLIC PRIVATE PARTNERSHIP

EPSRC Engineering and Physical Sciences Research Council

Thank you for your attention!

L, Pérez-Liva, Treeby, Cox, 2020. Time-Domain Full Waveform Inversion for High Resolution 3D Ultrasound Computed Tomography of the Breast, *in preparation.*

Fonseca, Malone, L, Ellwood, An, Arridge, Beard, Cox, 2017. Three-dimensional photoacoustic imaging and inversion for accurate quantification of chromophore distributions, *Proc. SPIE 2017.*

PHOTONICS PUBLIC PRIVATE PARTNERSHIP

EPSRC Engineering and Physical Sciences Research Council